



Attachment of noble metal nanoparticles to conducting polymers containing sulphur – preparation conditions for enhanced electrocatalytic activity

V.C. Ferreira^{a,b}, A.I. Melato^a, A.F. Silva^b, L.M. Abrantes^{a,*}

^a CQB, Departamento de Química e Bioquímica, Faculdade de Ciências da Universidade de Lisboa, Campo Grande, 1749-016 Lisboa, Portugal

^b CIQ-UP, Linha 4, Departamento de Química, Faculdade de Ciências da Universidade do Porto, Rua do Campo Alegre 687, 4169-007 Porto, Portugal

ARTICLE INFO

Article history:

Received 25 June 2010

Received in revised form 9 November 2010

Accepted 10 November 2010

Available online 18 November 2010

Keywords:

Gold and platinum nanoparticles

Electropolymerization

Sulphur-containing polymers

Electrocatalytic oxidation

Hydrazine

ABSTRACT

Taking advantage of the spontaneous deposition of noble metals on polymers containing sulphur, the inclusion of gold and platinum in poly(3-methylthiophene) and poly(3,4-ethylenedioxythiophene) (PEDOT) layers, achieved by immersion of the polymer into the metal nanoparticles suspension, is reported in the present work.

Platinum and gold nanoparticles (NPs), with diameters between 3 and 17 nm, have been prepared from colloidal methods (citrate or borohydride reduction in the presence of citrate capping agent) and characterized by transmission electron microscopy, ultraviolet–visible spectrophotometry and X-ray diffraction (XRD). The electropolymerization was carried out under potentiostatic and potentiodynamic conditions, imparting distinct morphologies, as revealed by atomic force microscopy. After polymer films immersion in the colloidal solutions, evidence of the NPs confinement and distribution was provided by XRD analysis and scanning electron microscopy. For thin layers, the quantity of attached metal NPs could be estimated from quartz crystal microbalance data collected throughout the films immersion. The influence of the polymer type and morphology, NPs nature, size and incorporated amount on the electrocatalytic activity of the so-prepared modified electrodes towards the hydrazine oxidation, in phosphate buffer solution, has been investigated by cyclic voltammetry. The results clearly show the superior properties of potentiodynamically prepared PEDOT films attaching very small (3 nm) freshly prepared Pt-NPs.

© 2010 Elsevier Ltd. All rights reserved.

1. Introduction

Particular attention has been paid to the synthesis of conducting polymer (CP) films embedding noble metal nanoparticles (NPs), due to potential applicability of these composite materials in a wide range of fields [1]. They exhibit interesting electrocatalytic properties due to the combination of the porous structure and high efficiency for the flow of electronic charges of CPs, with the high reactive surface area displayed by noble metal NPs [2,3].

The incorporation of noble metal NPs onto CP modified electrodes is well documented. Widely used routes have been the spontaneous chemical reduction of metal ions from their salt solution at the CP/solution interface (electroless precipitation) [4,5] and the metal electrochemical deposition [2,3,6,7]. However, the primarily deposition at the surface of the polymer film and the formation of irregularly shaped metal particles (Me-NPs) are recognized unsolved problems in both procedures [8]. A reported alternative is the trapping of metallic anions into the CP films during its electrochemical preparation followed by cathodic reduction

[9], but more recent approaches rely on the inclusion of pre-synthesised NPs [10–12].

Stabilized Me-NPs have been incorporated into CP films during the electropolymerization step [12,13] or through physical adsorption/chemical bonding [14], taking advantage of the spontaneous deposition of noble Me-NPs on polymers containing sulphur in their heterocyclic structures. The latter is an extremely simple method just requiring the polymer films dipping into the NPs containing colloidal solutions for a given period; it has been firstly reported for the attachment of Ag- and Au-NPs in potentiostatically prepared poly(3-methylthiophene) (P(3-MeTh)) and poly(3,4-ethylenedioxythiophene) (PEDOT) films, and demonstrated that contacts between the metal particles and the polymeric materials are ohmic [14]. It can be anticipated that other Me-NPs can be successfully used to build such type of platforms.

In spite of the high catalytic activity for the oxidation of several substrates claimed for Pt-modified polymer film electrodes [13,15–17], to the best of our knowledge the interaction of Pt-NPs with thiophene derivatives have not been attempted.

In the present work, such attractive route is exploited to attach Pt-NPs to PEDOT and P(3-MeTh) films and the characteristics of the so-obtained modified electrodes are compared with those observed for same polymers bearing Au-NPs.

* Corresponding author. Tel.: +351 21750000; fax: +351 21750088.

E-mail address: luisa.abrantes@fc.ul.pt (L.M. Abrantes).

Pristine P(3-MeTh) is inactive towards hydrazine oxidation. Although a non-negligible response is displayed by PEDOT to that important reaction, it has been chosen to examine the electrocatalytic properties of the prepared composites. As reported [18], a decrease in activity with the increase of the NPs size has been observed for AuNPs-deposited P(3-MeTh); when small sized Au and Pt particles (3–5 nm) are used, the best catalytic behaviour is exhibited by Pt-NPs modified films; among the two polymers, PEDOT appears as more efficient sulphur-containing matrix to append the noble metal NPs.

Being well known that the polymer properties, namely the porosity and the morphology, are imparted by the electrosynthesis parameters [19,20], it is predictable that the arrangement of sulphur atoms on the film surface is also dependent on the employed electropolymerization mode and conditions. Since the attachment of Au and Pt nanoparticles results from a linkage with surface available sulphur atoms, this aspect is relevant for electrocatalysis purposes and has also been considered in the present work.

2. Experimental

2.1. Synthesis and characterization of PEDOT and P(3-MeTh)

3,4-Ethylenedioxythiophene, EDOT (Aldrich), was distilled under reduced pressure prior to use and 3-methylthiophene, 3-MeTh (Aldrich), was used as received. Acetonitrile, ACN (HPLC grade, Aldrich 99.93%), was previously dried in calcium hydride and distilled with phosphorus pentoxide under N_2 atmosphere. Tetra-butylammonium perchlorate, TBAClO₄ (Fluka, puriss. $\geq 99\%$), was previously recrystallized from ethanol.

A polycrystalline platinum working electrode was used in all conventional electrochemical experiments. Before each experiment a fresh mirror-finish surface was generated by hand-polishing in an aqueous suspension of successively finer grades of alumina (from 5 to 0.05 μm). For other analysis, platinum-coated slides ($1.1 \times 1.1 \text{ cm}^2$, Arrandee, GmbH) working electrodes were utilized. These substrates were cleaned in “piranha” solution for a few minutes, rinsed with water and dried under a nitrogen flow. A Pt foil and a saturated calomel electrode (SCE, 0.244 V vs SHE) were used as counter and reference electrode, respectively.

From 20 mmol dm^{-3} EDOT in 0.1 mol dm^{-3} TBAClO₄ acetonitrile solution, the potentiostatic polymerization was carried out at a 1.20 V ($E_g = 1.20 \text{ V}$) up to a growth charge (Q_g) of ca. 30 mC cm^{-2} ; the working electrode potential was first switched from 0 to 0.845 V and held for 10 s to allow the double-layer charging of the Pt | solution interface, aiming to minimize the distortion of the polymerization current transient [21], and then a second potential pulse from 0.85 V to the growth potential, E_g , applied. The potentiodynamic deposition of PEDOT was carried out by cycling the potential between –0.8 and +1.18 V for the first five cycles, then lowering the anodic limit to 1.16 V for the next three cycles, and to 1.15 V for the following cycles (22), at 50 mV s^{-1} sweep rate. The total number of potential cycles was chosen in order of observing PEDOT films with similar oxidation charge to those prepared potentiostatically (ca. 10 mC cm^{-2}).

P(3-MeTh) films were prepared from 20 mmol dm^{-3} monomer in 0.1 mol dm^{-3} TBAClO₄ acetonitrile solution, potentiostatically at $E_g = 1.420 \text{ V}$, with Q_g of ca. 90 and 160 mC cm^{-2} , as well as by potential cycling, from 0.0 V to 1.450 V, at 50 mV s^{-1} ; with seven and eleven cycles, the polymer layers display oxidation charges similar to P(3-MeTh) deposited at constant potential.

The films were electrochemically characterized in monomer free solutions, at $\nu = 50 \text{ mV s}^{-1}$. Prior to the measurements, the solutions were de-aerated by bubbling N_2 (high purity, dried) for 20 min. The electrochemical experiments were performed with

an IMT electrochemical interface and a DEA332 digital electrochemical analyser connected to a computer for data acquisition (VoltaMaster2 software).

Polymers surface morphology has been assessed by AFM utilizing a Nanoscope IIIa multimode microscope (Digital Instruments, Veeco) equipped with the extended electronics module for topographic and phase imaging. The images were obtained in air, in *tapping* mode using etched silicon tips with a resonance frequency of ca. 300 kHz (Budgetsensors Tap300), and with a scan rate of 1.0–1.5 Hz.

2.2. Synthesis and characterization of Au- and Pt-NPs

Gold particles of 15–20 nm average diameter were synthesised through the Turkevich method [22,23]. Small sized (3–5 nm) citrate/Au-NPs and citrate/Pt-NPs have been synthesised through a sodium borohydride (NaBH_4) reduction method at room temperature, in agreement with a previously reported method [24], slightly modified to 20 mL of an aqueous solution containing $1.25 \times 10^{-4} \text{ mol dm}^{-3}$ HAuCl_4 (or K_2PtCl_6 , BDH Chemicals) and $2.5 \times 10^{-4} \text{ mol dm}^{-3}$ sodium citrate dihydrate, 300 μL of ice-cold 0.01 mol dm^{-3} NaBH_4 (Merck, p.a.) was rapidly added. The solutions were stirred for 30–60 s and then stand for ca. 15 min before stored in the dark at 4 °C.

The Au-NPs and Pt-NPs were characterized by UV–vis spectrophotometry (UV–vis, Jasco V560 spectrophotometer), transmission electron microscopy (TEM, Hitachi H-8100 transmission electron microscope, operating at 10–15 kV) and X-ray diffraction analysis (XRD, Philips – PW 1710 diffractometer with Cu $K\alpha$ radiation ($\lambda = 0.15418 \text{ nm}$) operated at 40 kV and 30 mA with a time per step of 5.000 s and step size of 0.005°).

2.3. Preparation and characterization of the modified electrodes

The confinement of the NPs on the polymers was performed by dipping the films in the NPs suspensions for 25 min or 5 h. The presence of the NPs in the polymeric layers was analysed by XRD under the above mentioned conditions.

A frequency analyser (CH Instruments model 420) was used to estimate the amount of deposited NPs; the experiments were performed in a single compartment cell. The working electrode was an 8 MHz AT-cut quartz crystal coated with 100 nm Pt (0.2 cm^2 geometrical area), previously cleaned with “piranha” solution and electrochemically by potential cycling in sulphuric acid solution, a Pt wire and a SCE were used as counter and reference electrodes, respectively.

The modified electrodes (ME) were analysed by scanning electron microscopy (SEM) with a Hitachi-SU70 (HR-SEM-SE) system, operating at 10–15 kV.

Hydrazine dihydrochloride, $\text{NH}_2\text{NH}_2 \cdot 2\text{HCl}$ (Carlo Erba, p.a., $\geq 99\%$) in phosphate buffer (PB) solution, pH 7, prepared from sodium dihydrogen phosphate monohydrate, $\text{NaH}_2\text{PO}_4 \cdot \text{H}_2\text{O}$ (Merck, p.a., 99%) and di-sodium hydrogen phosphate anhydrous, Na_2HPO_4 (Merck, p.a., 99%), was employed to characterize by cyclic voltammetry the electrochemical behaviour of the ME. Ultra-pure Milli-Q water was used for the preparation of aqueous solutions.

3. Results and discussion

3.1. Polymer films preparation and characterization

PEDOT films were deposited on Pt electrodes under potentiodynamic and potentiostatic control, using previously defined conditions [20] for observing films displaying similar electroactivity, e.g., about 10 mC cm^{-2} oxidation charge (Q_{ox}) during the

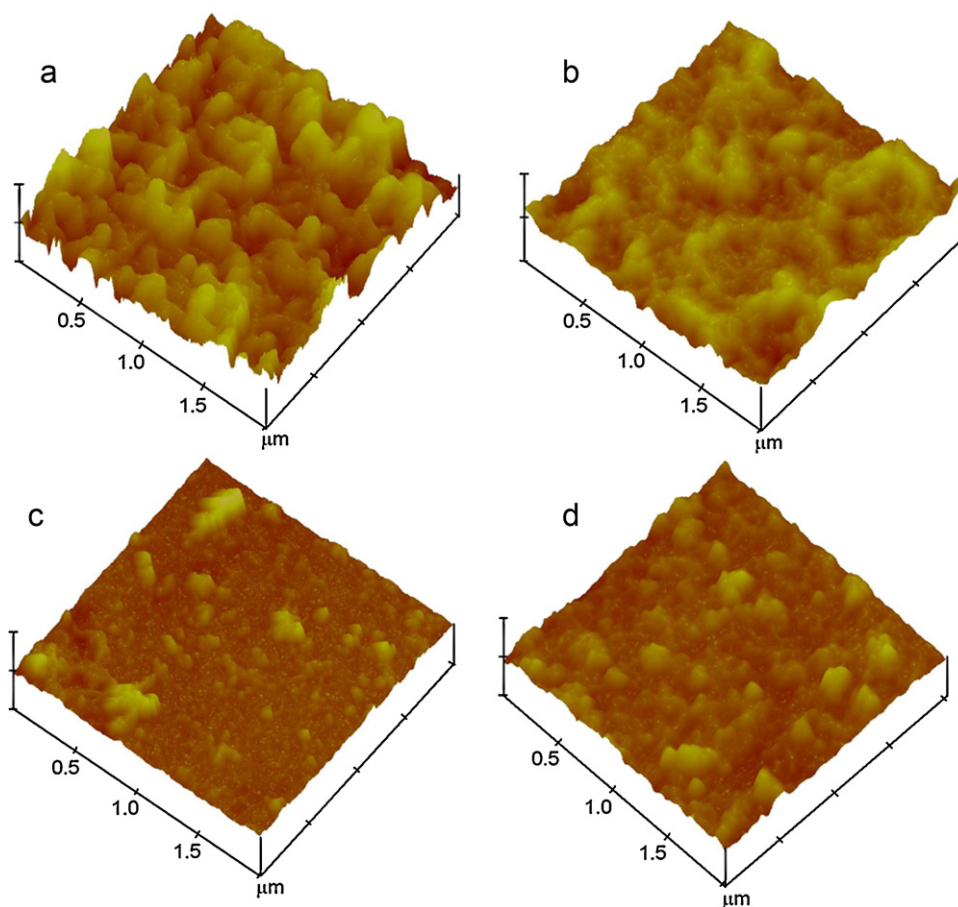


Fig. 1. *Ex situ* AFM images ($2 \times 2 \mu\text{m}^2$) of PEDOT grown potentiodynamically (30 potential cycles) (a) and at constant potential ($E_g = 1.20 \text{ V}$, $Q_g = 30 \text{ mC cm}^{-2}$) (b) and of P(3-MeTh) prepared by cyclic voltammetry (7 cycles) (c) and potentiostatically ($E_g = 1.42 \text{ V}$, $Q_g = 90 \text{ mC cm}^{-2}$) (d); $Z = 500 \text{ nm}$.

redox conversion in monomer free electrolyte solution. Notwithstanding, there is a difference in the magnitude of the redox peaks, namely in the relative intensity of the cathodic waves. The authors have recently reported [20,25] that these features are related to the preparative conditions; compared to the film deposited under constant potential, a more porous layer is formed by multiple potential cycles, where the egress of counter ions is easier.

The same methodology has been applied to the growth of P(3-MeTh) layers, with $Q_{ox} \approx 8 \text{ mC cm}^{-2}$; the cyclic voltammetric behaviour of such thin films reveals no noteworthy distinctions.

Fig. 1 shows the AFM morphological characterization of the polymer films. As expected [20], very rough surfaces are observed for PEDOT, Fig. 1(a and b), where the agglomeration of grains with diameters ranging from 60 to 160 nm is clearly dependent on the electropolymerization mode: fibber-like structures are observed in the potentiodynamically prepared film, whereas granules clustering characterizes that formed at constant potential. The respective root mean square (RMS) roughness values (R_q), 100 nm and 55 nm, reinforces the distinct surface morphologies. In contrast to PEDOT, the images of both P(3-MeTh) films, Fig. 1(c and d), expose dense and smooth initial layers, on the top of which new patterns come into sight, more markedly when the polymer is grown under potentiostatic control. Granules agglomeration is also noticeable during this second polymerization stage [26], and it can be anticipated that thicker layers would present much rougher surfaces. In the present case, the observed R_q values, 17 nm and 31 nm, respectively for the potentiodynamic and potentiostatically prepared P(3-MeTh), confirm that these films are much less porous than PEDOT.

3.2. Au- and Pt- NPs characterization

Fig. 2 depicts the UV–vis absorption spectra of the prepared colloids. The strong plasmon resonance absorption bands at about 522 nm and 516 nm, observed for the reddish and pink Au-NPs containing solutions respectively, Fig. 2(a), denote the presence of small sized particles, with 14–20 nm and below 9 nm, in agreement with reported values [24,27]. As can be seen in Fig. 2(b), the well defined absorption peak at ca. 260 nm due to Pt (IV) species is absent in the spectrum of the colloid obtained in the preparation of Pt-NPs, which confirms the formation of colloidal Pt [28].

Fig. 3 displays representative transmission electron microscopy (TEM) images and particle size histograms of the Au- and Pt-NPs used in this work. Rather uniformly sized spherical nanoparticles are observed in all cases. The particle size distribution has been obtained by direct measuring the size of ca. 300 randomly chosen particles in the several magnified TEM images prepared from the same colloidal solution. The analysis confirmed that the average diameter (ϕ) of the Au-NPs in the reddish colloidal solution is 15.1 nm whereas smaller particles ($\phi = 4.9 \text{ nm}$) are formed under different preparative conditions, namely by decreasing the metallic salt/reducing agent concentration ratio. With respect to the colloidal Pt, the data reveals that the average particle size is 3 nm.

The XRD patterns of the citrate-stabilized Au- and Pt-NPs deposited on amorphous silicon slides are depicted in Fig. 4. The crystalline nature of both gold samples (Fig. 4(a)) is evidenced by the diffraction peaks at 38.14° , 44.30° , 64.64° and 77.62° corresponding to the (1 1 1), (2 0 0), (2 2 0) and (3 1 1) facets, respectively [29]; the relative intensities of the peaks suggest the predominance of the (1 1 1) crystallographic orientation. Also crystalline and primar-

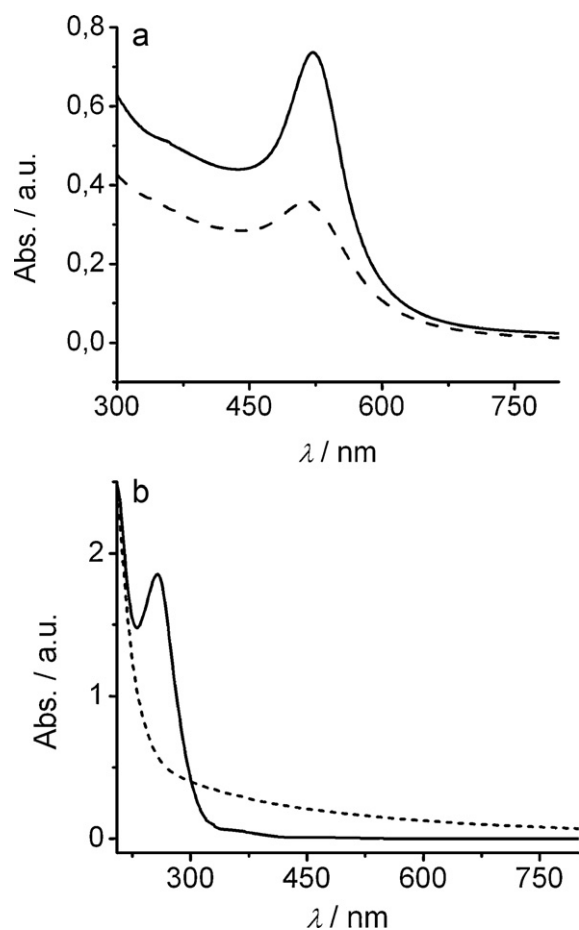


Fig. 2. UV-vis spectra of: (a) the reddish (—) and pink (---) colloidal suspensions of Au-NPs and (b) 0.12 mmol dm⁻³ K₂PtCl₆ solution (—) and colloidal Pt (---).

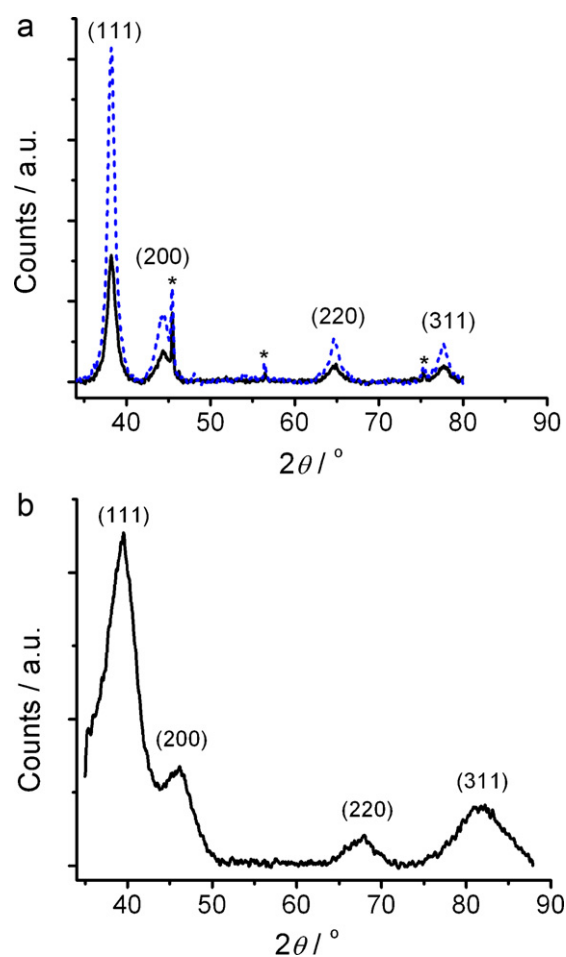


Fig. 4. X-ray patterns of: (a) Au-NPs with (—) $\phi \approx 5$ nm and (---) $\phi \approx 15$ nm and (b) Pt-NPs with $\phi \approx 3$ nm, deposited on amorphous silicon; diffraction lines from the reaction mixture marked with asterisk.

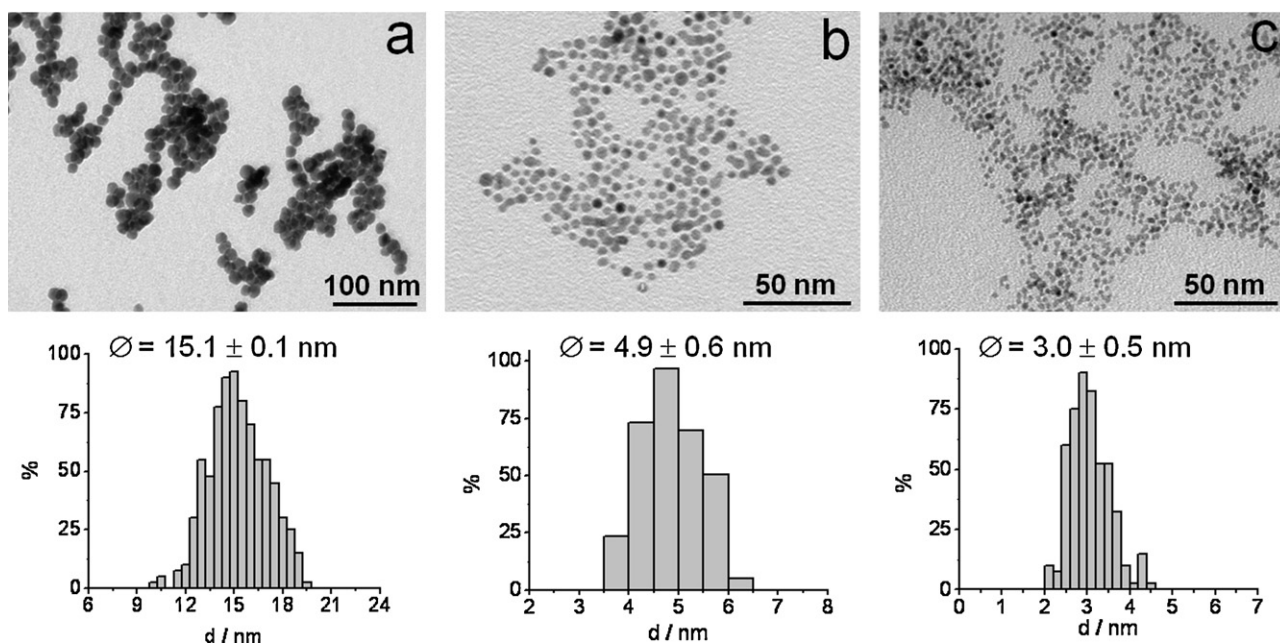


Fig. 3. Representative TEM micrographs and size distribution of Au-NPs with average diameter of: (a) 15 nm and (b) 5 nm and (c) Pt-NPs with average diameter of 3 nm.

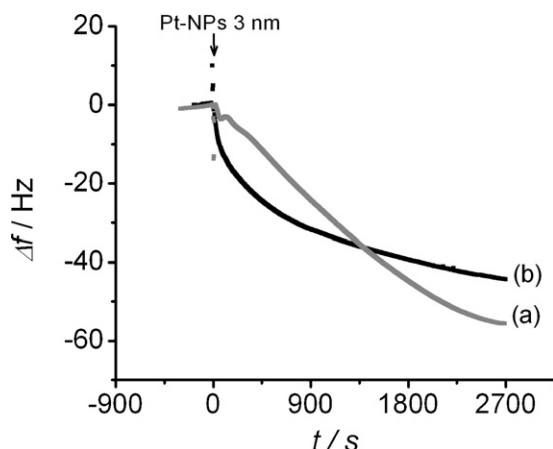


Fig. 5. Resonant frequency changes during the attachment of 3 nm Pt-NPs, from suspension with NPs concentration of ca. 73 nmol dm^{-3} , onto (a) PEDOT film grown under potentiostatic control, $E_g = 1.20 \text{ V}$, $Q_g = 5 \text{ mC cm}^{-2}$, and (b) P(3-MeTh) film grown under potentiostatic control, $E_g = 1.42 \text{ V}$, with $Q_g = 15 \text{ mC cm}^{-2}$.

ily dominated by the lowest energy (1 1 1) facets are the deposited Pt-NPs, as attested by the analysis of the diffractogram shown in Fig. 4(b): relatively intense peak at 39.62° , and weaker peaks at 46.22 , 67.70 and 81.54° , toning the (1 1 1), (2 0 0), (2 2 0) and (3 1 1) facets, correspondingly [30]. In Fig. 4, the additional diffraction peaks (indicated with an asterisk) are due to the presence of NaCl in the reaction mixture [31].

3.3. Au- and Pt-NPs attachment to the polymer films and characterization of composite modified electrodes

Attempting to access the amount of NPs that attaches to the polymer, Pt-coated quartz crystal electrodes have been used to deposit under potentiostatic control the P(3-MeTh) ($E_g = 1.42 \text{ V}$, $Q_g = 15 \text{ mC cm}^{-2}$, $Q_{ox} = 1.0 \text{ mC cm}^{-2}$) and PEDOT ($E_g = 1.20 \text{ V}$, $Q_g = 5 \text{ mC cm}^{-2}$, $Q_{ox} = 1.3 \text{ mC cm}^{-2}$) films and the change in frequency during their immersion into the 3 nm Pt-colloidal solution analysed using the Sauerbrey equation [32]. Taking into account that to a negative frequency shift of 1 kHz corresponds to an electrode-mass increase of 7 g cm^{-2} , from the data presented in Fig. 5 it is possible to retrieve the Pt-NPs loads. For 45 min immersion time, the mass increase of the P(3-MeTh) and PEDOT modified electrodes, is 0.30 and $0.39 \text{ } \mu\text{g cm}^{-2}$ respectively, which go with surface coverages of 26 and 35%.

It is noteworthy that after 1400 s both polymers present the same mass change ($0.25 \text{ } \mu\text{g cm}^{-2}$).

Due to experimental constraints (frequency change limit in the QCM), these essays employed polymer layers with rather different thickness and thus distinct morphologies/active areas should be considered in a deep analysis of the Pt-NPs up-loading course of action. However, since the AFM analysis (Fig. 1) of films displaying the same oxidation charge showed a higher roughness for PEDOT than for P(3-MeTh), it can be expected that the thinner films prepared for QCM experiments ($Q_{ox} \approx 1 \text{ mC cm}^{-2}$) would present a similar tendency, which is supported by the higher amount of attached Pt-NPs on PEDOT film after 45 min. Even so, it is worthwhile to note that the kinetics of the process appears to be rather different in the two films: during the first 1800 s, the almost linear augment in mass recorded for PEDOT, contrasts to the sharp initial (up to 200 s) increase observed for P(3-MeTh).

A further confirmation of the NPs attachment to the polymers has been achieved by XRD analysis of the composites prepared with $\varnothing \approx 15 \text{ nm}$ Au-NPs and PEDOT or P(3-MeTh), Fig. 6. In comparison to the pattern shown in Fig. 4(a), the peak at 77.62° and correspond-

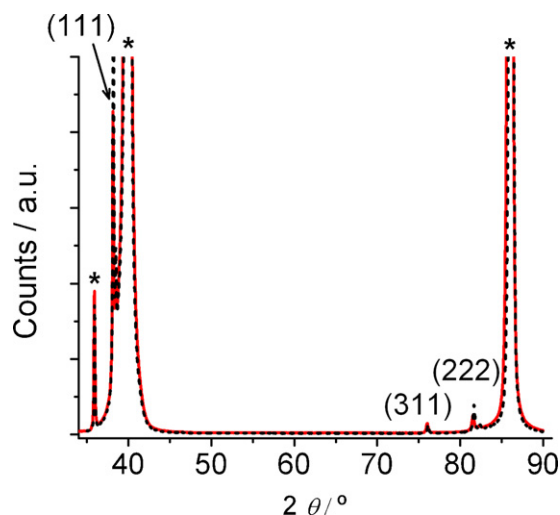


Fig. 6. X-ray diffraction patterns of PEDOT/Au-NPs (—) and P(3-MeTh)/Au-NPs (---) modified electrodes. Polymers grown under potentiostatic control, PEDOT: $E_g = 1.20 \text{ V}$, $Q_g = 140 \text{ mC cm}^{-2}$ and P(3-MeTh): $E_g = 1.45 \text{ V}$, $Q_g = 160 \text{ mC cm}^{-2}$ and immersed in the Au-NPs ($\varnothing \approx 15 \text{ nm}$) colloidal solution for 17 h; substrate diffraction lines marked with asterisk.

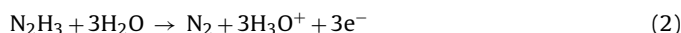
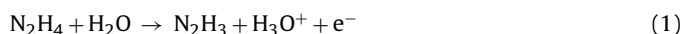
ing to (3 1 1) is much weaker and the diffraction peak of (2 2 0) plan, although detected in the results file at 64.79° , is not visible in the diffractogram, very likely due to the strong contribution of the substrate; also, the signal of (2 0 0) plan is not perceived, possibly owing to the different orientation that the nanoparticles adopt when immobilized in the polymers. However, the peak at 38.14° , is intense and well defined, supporting that the (1 1 1) facet is the preferential orientation of gold NPs in the composites.

To ascertain the influence of the base polymer film morphology on the amount/dispersion of the NPs, potentiodynamic and potentiostatically prepared PEDOT films were used to attach Au-NPs ($\varnothing \approx 15 \text{ nm}$). The morphology of modified electrodes has been characterized by scanning electronic microscopy (SEM) and the images are presented in Fig. 7.

A large quantity of particles homogeneously distributed on the polymer surface can be seen in both cases (Fig. 7(a and b)), in spite of the differences on the surface roughness of PEDOT prepared under distinct electrochemical modes. The Au-NPs appear to deposit as readily on the top of the thin fibers as on the large granules; as long as the sulphur atoms on the polymer surface are available, no significant differences can be detected in the composites morphologies.

3.4. Electrocatalytic behaviour towards hydrazine oxidation

Due to its relevance to chemical and pharmaceutical industries [33–35], the electrocatalytic oxidation of hydrazine (HZ) has been intensively studied [35,36]. In 5–10 pH range, it is generally accepted that the irreversible oxidation of hydrazine involves two steps [34,35], Eqs. (1) and (2), i.e., a single electron transfer (rate determining) followed by a 3-electron process to give N_2 as final product.



In the present work the electrocatalytic activity of the modified electrodes towards the oxidation of HZ in phosphate buffer solution has been investigated by voltammetry. The response of bare gold and platinum electrodes as well as of pristine P(3-MeTh) and PEDOT films is illustrated in Fig. 8 and the respective voltammetric features listed in Table 1. The superior performance exhibited

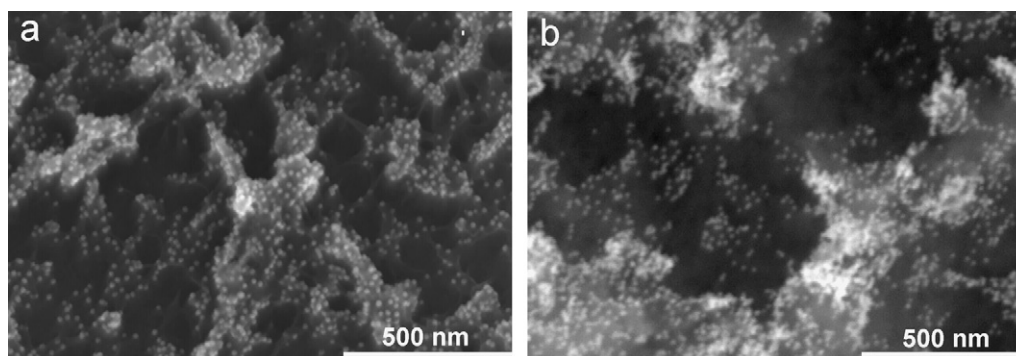


Fig. 7. Scanning electronic micrographs of PEDOT/Au-NPs modified electrodes. 2 h immersion time in Au-NPs ($\varnothing \approx 15$ nm) colloidal solution; polymer grown (a) potentiodynamically (50 mV s^{-1} , 30 cycles) and (b) potentiostatically ($E_g = 1.20 \text{ V}$, $Q_g = 30 \text{ mC cm}^{-2}$).

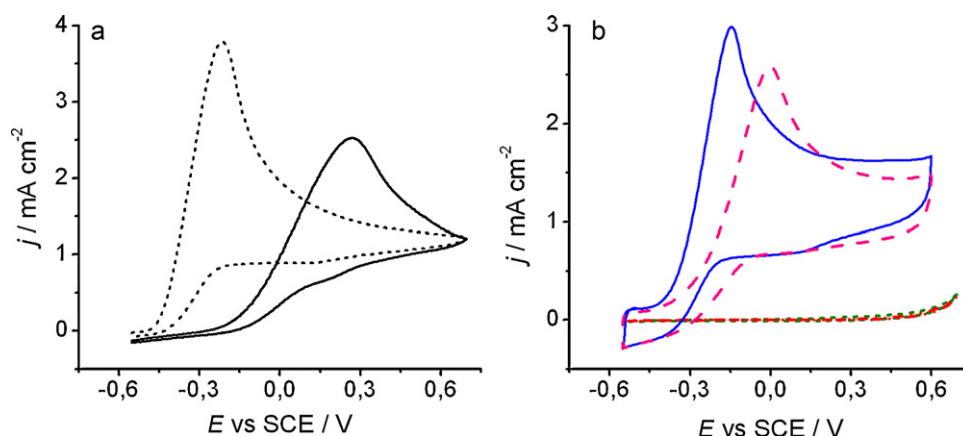


Fig. 8. Cyclic voltammograms of polycrystalline Au (—) and Pt (---) electrodes (a) and polymer modified electrodes (b): PEDOT (prepared potentiostatically, $E_g = 1.20 \text{ V}$, $Q_g \approx 28 \text{ mC cm}^{-2}$) (—); PEDOT (grown potentiodynamically, $\nu = 50 \text{ mV s}^{-1}$, 30 cycles) (—); P(3-MeTh) (deposited potentiostatically, $E_g = 1.42 \text{ V}$, $Q_g \approx 90 \text{ mC cm}^{-2}$) (●●●●●); P(3-MeTh) (prepared potentiodynamically, $\nu = 50 \text{ mV s}^{-1}$, 7 cycles) (●●●●●), at 50 mV s^{-1} scan rate, in 6 mmol dm^{-3} hydrazine in 0.1 mol dm^{-3} PB solution.

by bulk Pt has already been reported [37]; in comparison to gold, a much lower onset potential and a remarkably higher current as function of the applied potential are observed on Pt electrodes (Fig. 8(a)). A pretty similar behaviour is achieved with PEDOT film electrodes, being clearly advantageous to prepare the polymer under potentiostatic control (Fig. 8(b)). In great contrast is the inactivity of P(3-MeTh), displaying a near nule faradaic current up to 0.6 V.

Being inactive for the process under investigation, potentiostatically prepared P(3-MeTh) has been used to analyse, by cyclic voltammetry, the electrocatalytic response of the composites and its dependence on different experimental parameters, such as the

Table 1

Current peak potentials (vs. SCE) and respective current densities for the oxidation of hydrazine (6 mmol dm^{-3} in 0.1 mol dm^{-3} PB solution) on bulk gold and platinum electrodes and on pristine PEDOT and P(3-MeTh) modified electrodes, evaluated from the voltammograms shown in Fig. 8.

Electrode	$j_{\text{ox, pk}}/\text{mA cm}^{-2}$	$E_{\text{ox, pk}}/\text{mV}$
Au	2.5	270
Pt	3.8	−248
P(3-MeTh) ^a	—	—
PEDOT ^b	3.0	−148
PEDOT ^c	2.0	6

^a P(3-MeTh) films prepared under potentiostatic control ($E_g = 1.42 \text{ V}$, $Q_g \approx 90 \text{ mC cm}^{-2}$).

^b PEDOT film prepared under potentiostatic control ($E_g = 1.20 \text{ V}$, $Q_g \approx 28 \text{ mC cm}^{-2}$).

^c PEDOT film prepared under potentiodynamic control (50 mV s^{-1} , $[-0.8; 1.18] \text{ V}$, 30 cycles).

particle size and nature (Fig. 9(a and b)) as well as surface coverage, assuming its increase with the time of polymer immersion in the NPs containing solution (Fig. 9(c)); the effect of using freshly prepared or older than 3 weeks colloidal solutions has also been appraised (Fig. 9(d)). The route to reach the optimal conditions in preparing such type of composite electrode materials is plainly expressed by the voltammetric features along with the values of current peak potentials and respective current densities, summarized in Table 2. The oxidation peak potential decreases to less than one half of its value and the current peak density increases to almost the double, when gold nanoparticles with 15 nm are substituted by those with 5 nm diameter, revealing beneficial effect of using small sized particles; replacing the small Au nanoparticles by Pt particles of about the same size, a remarkable decrease in the oxidation potential is observed; for lowering the oxidation potential, a careful selection of the immersion time appears crucial: the

Table 2

Current peak potentials (vs. SCE) and respective current densities for the oxidation of hydrazine (6 mmol dm^{-3} in 0.1 mol dm^{-3} PB solution) on Au- and Pt-NPs/P(3-MeTh) modified electrodes, evaluated from the voltammograms shown in Fig. 9.

t_{imob}/h	Me-NPs (\varnothing)	$j_{\text{ox, pk}}/\text{mA cm}^{-2}$	$E_{\text{ox, pk}}/\text{mV}$
5	Au-NPs (5 nm)	4.0	232
5	Au-NPs (15 nm)	2.7	554
5	Pt-NPs (3 nm)	3.1	−54
25 min	Pt-NPs (3 nm)	2.5	220
5	Aged Pt-NPs (3 nm)	1.9	613

P(3-MeTh) films prepared under potentiostatic control ($E_g = 1.42 \text{ V}$, $Q_g \approx 90 \text{ mC cm}^{-2}$).

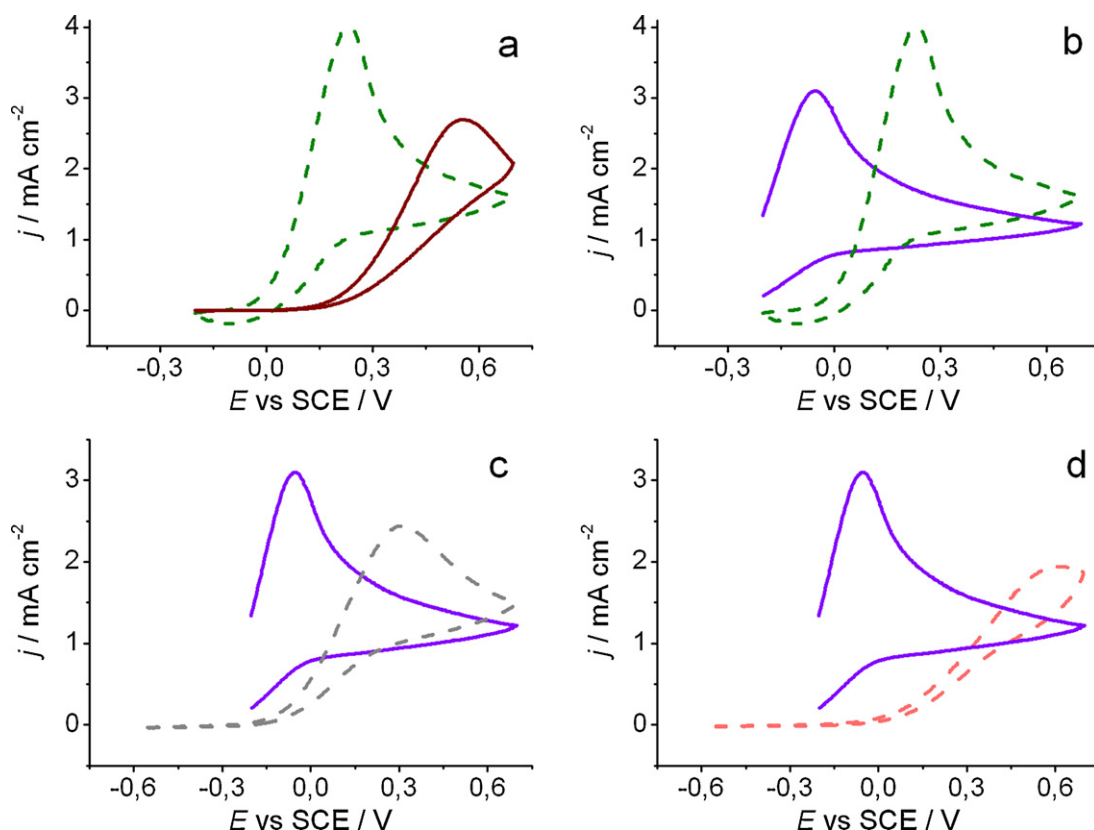


Fig. 9. Cyclic voltammograms of P(3-MeTh)/Me-NPs modified electrodes obtained upon immersion in freshly prepared colloidal solution of: Au-NPs with (—) $\varnothing = 15$ nm (5 h), (---) $\varnothing = 5$ nm (5 h), Pt-NPs with $\varnothing = 3$ nm (—) (5 h), (---) (25 min) and (---) aged Pt-NPs (5 h), in 6 mmol dm^{-3} hydrazine in 0.1 mol dm^{-3} PB solution at $\nu = 50 \text{ mV s}^{-1}$. P(3-MeTh) films potentiostatically prepared at $E_g = 1.42 \text{ V}$ with $Q_g \approx 90 \text{ mC cm}^{-2}$.

amount of attached Pt-NPs during 25 min is not enough to convey a good electrocatalytic response, since the amount of attached nanoparticles has not attained its maximum, as revealed by the QCM frequency evolution during the Pt-NPs confinement (Fig. 5). Also of relevance is to make use of fresh colloidal solutions. Probably in more than 3 weeks-old solutions, nanoparticles agglomeration and/or other reaction with the stabilizing agents occur, resulting in a non-effective interaction with the sulphur atoms of the polymer.

By attaching small sized Pt nanoparticles ($\varnothing = 3$ nm) to PEDOT, modified electrodes displaying excellent electrocatalytic activity

Table 3

Current peak potentials (vs. SCE) and respective current densities for the oxidation of hydrazine (6 mmol dm^{-3} in 0.1 mol dm^{-3} PB solution) on Au- and Pt-NPs/PEDOT modified electrodes, evaluated from the voltammograms shown in Fig. 10.

Polymer growth	Me-NPs (\varnothing)	$j_{\text{ox, pk}}/\text{mA cm}^{-2}$	$E_{\text{ox, pk}}/\text{mV}$
Consecutive potential cycling, $\nu = 50 \text{ mV s}^{-1}$	Pt-NPs (3 nm)	3.6	−275
Constant potential $E_g = 1.20 \text{ V}$	Pt-NPs (3 nm)	4.1	−255
	Au-NPs (5 nm)	2.7	−175
		2.4	175

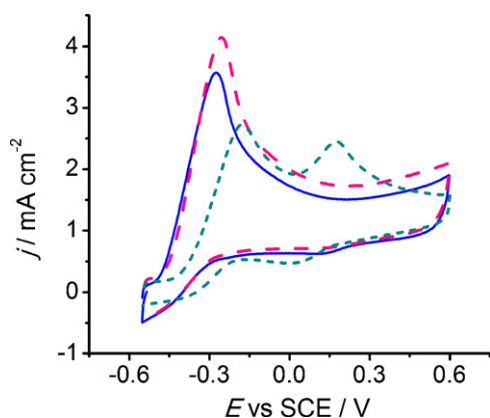


Fig. 10. Cyclic voltammograms in 6 mmol dm^{-3} hydrazine in 0.1 mol dm^{-3} PB solution of PEDOT/Pt-NPs ($\varnothing = 3$ nm) modified electrodes, obtained upon 5 h immersion in freshly prepared colloidal solution, being the polymer prepared under potentiodynamic control (50 mV s^{-1} , 30 cycles) (—) and under potentiostatic control ($E_g = 1.20 \text{ V}$, $Q_g \approx 28 \text{ mC cm}^{-2}$) (—). PEDOT/Au-NPs ($\varnothing = 5$ nm) formed at constant potential (---).

towards the oxidation of HZ are built, as exposed by the data shown in Fig. 10 and Table 3. The onset potential occurs at rather negative values and significant currents develop thereafter. It is noteworthy that for composites with the polymer grown under consecutive potential cycling, slightly lower onset potential and current peak potential are observed, in comparison to those prepared with polymer layers deposited under potentiostatic control.

The current response of PEDOT modified by the attachment of Au-NPs ($\varnothing = 5$ nm), displays two oxidation waves, Fig. 10; the one at more negative potential value suggests that the presence of the NPs slightly enhances the electrocatalytic performance of the unaltered polymer (see Fig. 8(b)) while the second is likely the result of HZ oxidation at the Au-NPs surface (see Fig. 8(a)). Obviously such behaviour is not interesting for electrocatalytic purposes.

4. Conclusions

Based on the strong interaction of noble metal particles with the sulphur atoms of thiophene derivatives, platinum or gold nanoparticles-dispersed polymers films have been successfully prepared.

Under the conditions employed in this work, spherical Au-NPs (5 and 15 nm diameter) and Pt-NPs (3 nm diameter) have been prepared, as confirmed by the physicochemical characterization of the NPs containing colloidal solution (UV–vis, TEM, XRD). As synthesised, the Au- and Pt-NPs are crystalline with (1 1 1) facets as predominant orientation and such characteristics are still observed after their attachment to the polymers films.

The simple immersion of electrochemically prepared P(3-MeTh) and PEDOT in Au or Pt colloid solution provided a uniform distribution of individualized nanoparticles on the polymer surface, without NPs aggregation, contrarily to the reported by other preparations methods [38]. Although highly dependent on the particle nature and size as well as on the polymer nature and morphology imparted by the electropolymerization mode and conditions, a surface coverage of 30% can be achieved, as shown for the attachment of small sized Pt-NPs to potentiostatically deposited PEDOT.

The cyclic voltammetric behaviour of these novel modified electrodes towards the hydrazine oxidation in PB solution has revealed a considerable enhancement in electrocatalytic activity, compared to polycrystalline Au or Pt electrodes and to pristine polymers. From the data it has also been possible to retrieve the composite preparative conditions required to reach an optimal activity. Besides the superior performance of Pt and pristine PEDOT, other crucial parameters are (i) the NPs size (when the size of the immobilized NPs increases the oxidation current decreases and the oxidation potential is shifted to more positive potentials), (ii) the use of freshly prepared colloid solutions to avoid particles agglomeration/adsorption of reaction products) and (iii) the surface coverage, i.e. to assure a proper immersion time. Accordingly, the attachment of 3 nm Pt-NPs to PEDOT produced composites with excellent electrocatalytic properties; on composites using potentiodynamically deposited polymer, the electrocatalytic oxidation of hydrazine occurs at -0.275 V, which is ~ 30 mV less positive than the value for conventional Pt bulk electrodes.

Taking into account the reported PEDOT–Pt degradation processes [39], work is in progress to establish the storage conditions envisaging the long-time stability of the systems described in the present work.

Acknowledgements

V.C. Ferreira and A.I. Melato gratefully acknowledge the financial support from Fundação para a Ciência e a Tecnologia, scholarships SFRH/BD/30585/2006 and SFRH/BD/13899/2003.

References

- [1] B.C. Sih, M.O. Wolf, *Chem. Commun.* (2005) 3375.
- [2] X. Huang, Y. Li, Y. Chen, L. Wang, *Sens. Actuators B* 134 (2008) 780.
- [3] A. Mourato, S.M. Wong, H. Siegenthaler, L.M. Abrantes, *J. Solid State Electrochem.* 10 (2006) 140.
- [4] A. Mourato, A.S. Viana, J.P. Correia, H. Siegenthaler, L.M. Abrantes, *Electrochim. Acta* 49 (2004) 2249.
- [5] M. Ocypa, M. Ptasíńska, A. Michalska, K. Maksymiuk, E.A.H. Hall, *J. Electroanal. Chem.* 596 (2006) 157.
- [6] M. Ilieva, V. Tsakova, *Synth. Met.* 141 (2004) 281.
- [7] S. Harish, J. Mathiyarasu, K.L.N. Phani, V. Yegnaraman, *J. Appl. Electrochem.* 38 (2008) 1583.
- [8] V. Tsakova, *J. Solid State Electrochem.* 12 (2008) 1421.
- [9] M. Grzeszczuk, P. Poks, *Electrochim. Acta* 45 (2000) 4171.
- [10] C.R.K. Rao, D.C. Trivedi, *Catal. Commun.* 7 (2006) 662.
- [11] C. Zanardi, F. Terzi, L. Pigani, A. Heras, A. Colina, J. Lopez-Palacios, R. Seeber, *Electrochim. Acta* 53 (2008) 3916.
- [12] F. Terzi, C. Zanardi, V. Martina, L. Pigani, R. Seeber, *J. Electroanal. Chem.* 619–620 (2008) 75.
- [13] L. Pigani, G. Foca, K. Ionescu, V. Martina, A. Ulrici, F. Terzi, M. Vignali, C. Zanardi, R. Seeber, *Anal. Chim. Acta* 614 (2008) 213.
- [14] S.H. Cho, S.-M. Park, *J. Phys. Chem. B* 110 (2006) 25656.
- [15] F.-J. Liu, L.-M. Huang, T.-C. Wen, A. Gopalan, *Synth. Met.* 157 (2007) 651.
- [16] V. Selvaraj, M. Alagar, I. Hamerton, *J. Power Sources* 160 (2006) 940.
- [17] E. Antolini, E.R. Gonzalez, *Appl. Catal. A* 365 (2009) 1.
- [18] P. Kalimuthu, S.A. John, *J. Electroanal. Chem.* 617 (2008) 164.
- [19] F. Blanchard, B. Carré, F. Bonhomme, P. Biensan, H. Pagès, D. Lemordant, *J. Electroanal. Chem.* 569 (2004) 203.
- [20] A.I. Melato, A.S. Viana, L.M. Abrantes, *J. Solid State Electrochem.* 14 (2010) 523.
- [21] H. Randriamahazaka, V. Noël, C. Chevrot, *J. Electroanal. Chem.* 472 (1999) 103.
- [22] J. Turkevich, P.C. Stevenson, J. Hiller, *Discuss. Faraday Soc.* 11 (1951) 55.
- [23] J. Kimling, M. Maier, B. Okenve, V. Kotaidis, H. Ballot, A. Plech, *J. Phys. Chem. B* 110 (2006) 15700.
- [24] N.R. Jana, L. Gearheart, C.J. Murphy, *Langmuir* 17 (2001) 6782.
- [25] A.I. Melato, A.S. Viana, L.M. Abrantes, *Electrochim. Acta* 54 (2008) 590.
- [26] F. Chao, M. Costa, C. Tian, *Synth. Met.* 52 (1993) 127.
- [27] S. Link, M.A. El-Sayed, *J. Phys. Chem. B* 103 (1999) 4212.
- [28] Z. Tang, D. Geng, G. Lu, *J. Colloid Interf. Sci.* 287 (2005) 159.
- [29] X. Zou, E. Ying, S. Dong, *Nanotechnology* 17 (2006) 4758.
- [30] Z. Tang, D. Geng, G. Lu, *Mater. Lett.* 59 (2005) 1567.
- [31] K. Linnow, H. Juling, M. Steiger, *Environ. Geol.* 52 (2007) 317.
- [32] S. Bruckenstein, M. Shay, *Electrochim. Acta* 30 (1985) 1295.
- [33] G. Choudhary, H. Hansen, *Chemosphere* 37 (1998) 801.
- [34] J. Li, X. Lin, *Sens. Actuators B* 126 (2007) 527.
- [35] S.M. Golabi, H.R. Zare, *J. Electroanal. Chem.* 465 (1999) 168.
- [36] K. Asazawa, K. Yamada, H. Tanaka, M. Taniguchi, K. Oguro, *J. Power Sources* 191 (2009) 362.
- [37] V. Rosca, M.T.M. Koper, *Electrochim. Acta* 53 (2008) 5199.
- [38] S. Patra, N. Munichandraiah, *Langmuir* 25 (2009) 1732.
- [39] J.-F. Drillet, R. Dittmeyer, K. Jüttner, *J. Appl. Electrochem.* 37 (2007) 1219.